Identification of Yeast Cofilin Residues Specific for Actin Monomer and PIP_2 Binding†

Pauli J. Ojala, Ville Paavilainen, and Pekka Lappalainen*

Program in Cellular Biotechnology, Institute of Biotechnology, University of Helsinki, P.O. Box 56, 00014 Helsinki, Finland

Received September 6, 2001; Revised Manuscript Received October 26, 2001

ABSTRACT: Cofilin/ADF is a ubiquitous actin-binding protein that is important for rapid actin dynamics in vivo. The long α-helix (helix 3 in yeast cofilin) forms the most highly conserved region in cofilin/ADF proteins, and residues in the NH_2-terminal half of this α-helix have been shown to be essential for actin binding in cofilin/ADF. Recent studies also suggested that the basic residues in the COOH-terminal half of this α-helix would play an important role in F-actin binding. In contrast to these studies, we show here that the charged residues in the COOH-terminal half of helix 3 are not important for actin filament binding in yeast cofilin. Mutations in these residues, however, result in a small defect in actin monomer interactions. We also show that yeast cofilin can differentiate between various phosphatidylinositides, and mapped the $PI(4,5)P_2$ binding site by using a collection of cofilin mutants. The $PI(4,5)P_2$ binding site of yeast cofilin is a large positively charged surface that consists of residues in helix 3 as well as residues in other parts of the cofilin molecule. This suggests that cofilin/ADF proteins probably interact simultaneoulsy with more than one $PI(4,5)P_2$ molecule. The $PI(4,5)P_2$-binding site overlaps with areas that are important for F-actin binding, explaining why the actin-related activities of cofilin/ADF are inhibited by $PI(4,5)P_2$. The biological roles of actin and $PI(4,5)P_2$ interactions of cofilin are discussed in light of phenotypes of specific yeast strains carrying mutations in residues that are important for actin and $PI(4,5)P_2$ binding.

Cofilin/ADF[1] is a small actin-binding protein first isolated from chick embryo brain as a protein that promotes the disassembly of actin filaments (*1*). Cofilin/ADF proteins are both ubiquitous and abundant in eukaryotes, and they regulate actin dynamics in vivo by increasing the rate of actin filament depolymerization (*2*−*4*). Proteins of the cofilin/ADF family also play an important role during cytokinesis (*5*, *6*) and cell motility (*7*), and they are essential for viability at least in *Saccharomyces cerevisiae* (*8*, *9*), *Dictyostelium discoideum* (*10*), *Caenorhabditis elegans* (*11*), and *Drosophila melanogaster* (*6*).

Cofilin/ADF binds both monomeric and polymeric actin with a 1:1 molar ratio with respect to actin monomers. Under physiological conditions, cofilin/ADF has a higher affinity for ADP-bound actin monomers and filaments than for ATP-bound ones (*12*, *13*). Cofilin/ADF binds to actin filaments in a highly cooperative manner, and this interaction is pH-dependent for most ADF/cofilins (*14*, *15*). Furthermore, recent electron microscopy studies by Galkin et al. (*16*) suggest that cofilin/ADF binds to actin filaments with a 2:1 (cofilin/ADF:actin) molar ratio (*16*). When bound to an actin filament, cofilin/ADF increases the twist of the filaments (*17*), and stimulates actin dynamics by depolymerizing F-actin from the pointed/minus ends, which is the rate-limiting step in the actin filament treadmilling cycle (*2*). Cofilin/ADF proteins also have a weak actin filament severing activity, and this may promote a generation of new barbed ends at the leading edge of motile cells (*18*−*20*). However, other studies suggested that cofilin/ADF does not sever filaments, but changes their thermodynamic parameters, which may account for its effects on the viscosity of actin filament solutions (*2*).

Actin binding and depolymerization activities of cofilin/ADF are negatively regulated by phosphoinositides (*21*). Cofilin seems to differentiate between phosphatidylinositol lipids, but the biological relevance of the PIP_2 interactions is still controversial (*22*, *23*). At least in higher eukaryotes, the actin interactions of cofilin/ADF can also be down-regulated by phosphorylation at a serine residue near the N-terminus of the protein (*24*).

NMR and crystal structures of cofilin/ADF family proteins have shown that, despite the lack of detectable sequence homology, these proteins fold into a tertiary structure strikingly similar to that of the repeated segments in the gelsolin family of actin filament severing/capping proteins (*25*−*27*). On the basis of the structural similarity between cofilin/ADF and gelsolin family proteins, it was suggested that cofilin/ADF would interact with G-actin in a manner

† This work was supported by grants from the Academy of Finland and Biocentrum Helsinki (to P.L.). P.J.O. is supported by a fellowship from the Viikki Graduate School of Biosciences.

* To whom correspondence should be addressed. Phone: +358-9-19159499. Fax: +358-9-19159366. E-mail: pekka.lappalainen@helsinki.fi.

[1] Abbreviations: ADF, actin depolymerizing factor; DTT, dithiothreitol; DMSO, dimethyl sulfoxide; PBS, phosphate-buffered saline; EGTA, ethylene glycol bis(β-aminoethyl ether)-*N*,*N*,*N*′,*N*′-tetraacetic acid; SDS−PAGE, sodium dodecyl sulfate−polyacrylamide gel electrophoresis; IP_3 or Ins1,4,5-P_3, inositol 1,4,5-trisphosphate; PI, phosphatidylinositol; PS, phosphatidylserine; PE, phosphatidylethanolamine; PC, phosphatidylcholine; PIP or PI(4)P, phosphatidylinositol 4-monophosphate; $PI(3,4)P_2$, phosphatidylinositol 3,4-diphosphate; PIP_2 or $PI(4,5)P_2$, phosphatidylinositol 4,5-diphosphate; $PI(3,4,5)P_3$, phosphatidylinositol 3,4,5-diphosphate; ϵ-ATP, etheno-ATP.

10.1021/bi0117697 CCC: $20.00
Published on Web 11/30/2001

similar to that of gelsolin segment 1 (*25*). To map the actin-binding surfaces of cofilin/ADF, we recently carried out a systematic mutagenesis on a yeast cofilin gene. By examining the biochemical defects of the mutants that resulted in a lethal or temperature sensitive phenotype in yeast, we identified five clusters of charged residues that are important for actin interactions in yeast cofilin. Three of these mutants led to defects in both actin monomer and actin filament binding, whereas two mutants resulted in defects in only actin filament interactions, without detectable defects in actin monomer binding (*28*). Other studies also have suggested that residues in the COOH-terminal region of the long α-helix of cofilin/ADF (helix 3 in yeast) would be crucial for actin filament interactions (*29*, *30*). However, in addition to the mutation at the NH_2-terminal end of helix 3, other mutations along the long α-helix of cofilin do not result in an altered growth phenotype in yeast (*28*). The lack of a detectable growth phenotype in yeast indicates that these COOH-terminal residues are not involved in actin filament binding in cofilin, or that the actin filament binding and depolymerization activities are not essential functions of cofilin.

In this study, we used site-directed mutagenesis to evaluate the role of the COOH-terminal region of the helix 3 of yeast cofilin in actin interactions. We show that the most highly conserved charged residues in this area of cofilin are not important for actin filament binding. However, a mutation in this area results in a small defect in actin monomer binding and sequestering. We also show that residues in this long α-helix, as well as residues in the other parts of cofilin, are involved in interactions with $PI(4,5)P_2$.

EXPERIMENTAL PROCEDURES

Site-Directed Mutagenesis and Plasmid Construction. The site-directed mutations were introduced into yeast cofilin cDNA by using the PCR-based overlap extension method (*31*). The oligonucleotides used in amplification created *Bam*HI and *Eco*RI sites at the 5′- and 3′-ends of the final PCR fragments, respectively. These fragments were ligated into a *Bam*HI−*Eco*RI-digested pGEX2T plasmid backbone as described in ref *28* to create plasmids pPL69, pPL70, and pPL121. Constructs were then sequenced by the chain termination method to verify the correct sequence.

Protein Expression and Purification. Yeast wild-type and mutant cofilins were expressed as glutathione *S*-transferase (GST) fusion proteins in *Escherichia coli* DH5α cells under the control of the P_{lac} promoter. Cells were grown in 1000 mL of LB medium to an optical density of 0.5 at 600 nm, and expression was induced with 0.4 mM isopropyl thio-β-D-galactoside (IPTG). Cells were harvested 3 h after induction, washed with 100 mL of 20 mM Tris (pH 7.5), resuspended in 20 mL of PBS, and lysed by sonication, after which the proteinase inhibitor phenylmethanesulfonyl fluoride (PMSF) was added to a final concentration of 0.15 mM. GST fusion proteins were enriched from the lysis supernatant by using glutathione−agarose beads (*32*). Cofilin−GST fusion proteins bound to glutathione−agarose beads were incubated overnight with thrombin (10 units/mL) at room temperature to cleave cofilin from GST. The beads were washed four times with 2 mL of 50 mM Tris (pH 7.5) and 150 mM NaCl. Supernatants were then pooled and concentrated in Centricon 10 kDa cutoff concentrators (Amicon Inc.) to 2 mL and loaded onto a Superdex-75 HiLoad gel exclusion chromatography column (Pharmacia Biotech) equilibrated with 10 mM Tris (pH 7.5) and 50 mM NaCl. The peak fractions containing cofilin eluted at ∼70 mL. Peak fractions were pooled, concentrated in Centricon 10 kDa cutoff devices to a final concentration of at least 100 μM, frozen in liquid N_2, and stored at −70 °C. Actin was purified from baker's yeast cell extract with a DNase I affinity column as described by Zechel (*33*), and modified by Rodal et al. (*34*), to decrease the level of cofilin contamination through a polymerization cycle at high KCl concentrations. Rabbit muscle actin was purified as described by Spudich and Watt (*35*).

Native Gel Electrophoresis Assays. Native polyacrylamide gel electrophoresis for studying protein−protein and protein−lipid interactions was performed as described by Safer et al. (*36*) and Gungabissoon et al. (*22*), respectively. After evaporation under N_2 gas, lipids were hydrated in reaction buffer A [10 mM Tris (pH 7.5), 1 mM EGTA, and 1 mM DTT] in the presence of 0.5% radical scavenging BHT (butylated hydroxytoluene) and vigorously tip-sonicated for 3 × 10 s on ice. Lipids were then mixed in a 5-fold molar excess with yeast cofilin in buffer A. The sample was then mixed 1:1 with native gel buffer B [25 mM Tris, 195 mM glycine (pH 8.8) with 2 mM ATP, 0.2 mM EGTA, and 0.5 mM DTT] using 5% sucrose or 20% glycerol as a loading buffer, and loaded on 6% polyacrylamide gels. Gels were run at 10 mA for 80 min in 50% buffer B, and proteins were visualized by Coomassie staining. The lipids were purchased from Sigma except for $PI(3,4)P_2$ and $PI(3,4,5)P_3$ which were purchased from Matreya Inc. All the other lipids were tissue extracted with heterogeneous fatty acid composition, but $PI(3,4)P_2$ and $PI(3,4,5)P_3$ were synthesized in dipalmitoyl form (C16:0, C16:0).

Cosedimentation Assays. For the F-actin cosedimentation assays, 40 μL aliquots of 0, 2.5, 3.75, or 5 μM yeast actin were prepared in G-buffer [20 mM Tris (pH 7.5), 0.2 mM ATP, 0.2 mM DTT, and 0.2 mM $CaCl_2$]. Actin was polymerized for 30 min by turning G-buffer into F-buffer by adding 5 μL of 10× polymerization initiation mix (20 mM $MgCl_2$, 10 mM ATP, and 1 M KCl) to the reaction mixture. Yeast cofilin in G-buffer (5 μL of a 10 μM solution) was added upon premade filaments, and the samples were incubated for 30 min. Reaction mixtures were then centrifuged in a Beckman Optima MAX ultracentrifuge in a TLA-100 rotor at 75 000 rpm for 30 min. Equal proportions of supernatants and pellets were fractionated on 13.5% SDS−PAGE gels, and proteins were visualized by Coomassie staining. For the sequestering assays, the protocol was essentially the same as that described above, except that the final concentrations of actin and cofilin were 1 and 2 μM, respectively. All experiments were carried out at room temperature.

Fluorometric Assays. The rate of nucleotide exchange of actin and its inhibition by cofilin was measured as described previously (*28*). In this assay, the extent of the replacement of the ATP with ϵ-ATP (etheno-ATP) was measured as the increase in the fluorescence signal. Actin (1.25 μM) and cofilin (0, 0.25, 0.5, 0.75, 1, 1.25, 2.5, 3.75, and 5.0 μM) in 40 μL of G-buffer [10 mM Tris (pH 7.5), 0.2 mM $CaCl_2$, 1 mM DTT, and 4 μM ATP] were mixed with 10 μL of 200 μM ϵ-ATP. The reaction was followed by a BioLogic MOS-250 fluorescence spectrophotometer at an excitation wave-

length of 360 nm and an emission wavelength of 410 nm. The experimental data were fitted using the single-exponential and simplex optimization procedure of Biokine software. The normalized values of the observed rates were analyzed using SigmaPlot software and fitted using the following equation assuming 1:1 stoichiometry:

$$E = \frac{1}{2}c + \frac{1}{2}z - \frac{1}{2}\sqrt{(c+z)^2 - 4z}$$

where

$$z = \frac{[\mathrm{Cof}]_{\mathrm{tot}}}{[\mathrm{Act}]_{\mathrm{tot}}}$$

and

$$c = 1 + \frac{K_{\mathrm{d}}}{[\mathrm{Act}]_{\mathrm{tot}}}$$

The steady-state rate of rabbit muscle actin filament turnover was monitored as the decrease in the fluorescence of ϵ-ATP bound to F-actin after addition of ATP (*2*). ϵ-ATP-bound G-actin (20 μM) was polymerized at pH 8.0 in the presence of 100 μM ϵ-ATP. Samples (55 μL) of ϵ-ATP-bound F-actin were preincubated in the presence of 5 μM cofilin for 5 min, and the decrease in the fluorescence of ϵ-ATP (excitation at 350 nm, emission at 410 nm) was monitored with a BioLogic MOS-250 fluorometer after addition of 10 μL of 5 mM ATP.

Immunofluorescence Microscopy. Haploid yeast cells (DDY1252, DDY1263, and DDY1264) were grown in YEPD medium at 30 °C to an optical density of 0.5 at 600 nm. The cells were then prepared for immunofluorescence as described in ref *37*. The guinea pig anti-yeast actin serum was used at a 1:1000 dilution, and the rabbit anti-yeast cofilin antibody (*8*) was used at a 1:100 dilution. Actin and cofilin were then visualized with the FITC-conjugated goat anti-rabbit antibody (Jackson Laboratories) and the rhodamine-conjugated goat anti-guinea pig antibody (Jackson Laboratories), respectively.

Stability Studies. CD measurements were recorded with a Jasco spectropolarimeter (model J-700) equipped with a microcomputer and Jasco PTC-348WI thermostat. Spectra were collected with a scan speed of 50 nm/min, a step resolution of 0.5 nm, a bandwidth of 2.0 nm, a sensitivity of 20 mdeg, and a response time of 1 s. Each spectrum was the average of 12 scans. Far-UV CD spectra were recorded at a protein concentration of 3 μM [2 mM $NaPO_4$ (pH 7.4) and 25 mM UV-free NaCl (Aldrich)] with a 2 mm path length cell. For temperature transition studies, each scan at the desired temperature was recorded after an incubation time of 4 min and the disruption of α-helices was plotted at 222 nm.

Molecular Modeling. Images of cofilin were generated on a Silicon Graphics Indigo workstation running Insight II software (MSI Inc.). Atomic coordinates for cofilin were retrieved from the Protein Data Bank (1COF), and the conformation of the five flexible N-terminal residues was modeled by computing their energy minimum with the Discover program (MSI Inc.).

Miscellaneous. Polyacrylamide gel electrophoresis was carried out using the buffer system of Laemmli (*38*). Protein concentrations were determined with a Hewlett-Packard 8452A diode array spectrophotometer by using calculated extinction coefficients for yeast cofilin (ϵ = 15.9 mM^{-1} cm^{-1} at 280 nm) and yeast actin (ϵ = 26.6 mM^{-1} cm^{-1} at 290−320 nm). Protein distribution in SDS−PAGE gels was quantified by a Fluor-S MultiImager with Quantity One version 4.1.0 (Bio-Rad). Western blotting with the rabbit anti-yeast cofilin antibody was carried out as described by Moon et al. (*8*).

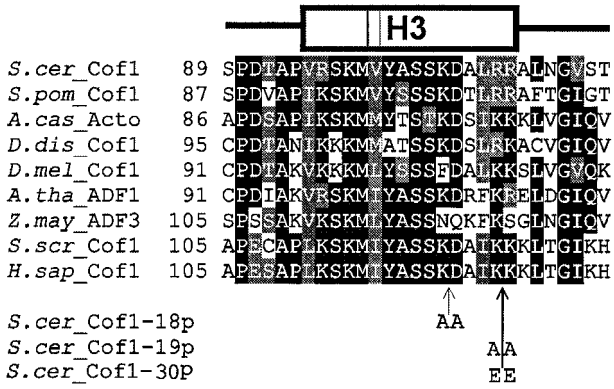

FIGURE 1: Multiple-sequence alignment of the long α-helix from representative cofilin/ADF proteins. The residues mutated in this study (K105 and D106 in Cof1−18p and R109 and R110 in Cof1−19p and Cof1−30p) are highly conserved and are located in the C-terminal part of the helix. Where no database is stated, the accession number refers to Swiss-Prot: *S. cerevisiae* cofilin, Q03048; *Schizosaccharomyces pombe* cofilin, P78929; *A. castellanii* actophorin, P37167; *D. discoideum* cofilin, P54706; *Dr. melanogaster* ADF, P45594; *Arabidopsis thaliana* ADF1, GenBank entry U48938; *Z. mays* ADF3, GenBank entry X97726; *S. scrofa* cofilin 1, P10668; and *Hono sapiens* cofilin 1, P23528.

RESULTS

The long α-helix (helix number 3 in yeast cofilin) forms the widest sequence conservation region between all of the known isoforms of the cofilin/ADF proteins in different species (Figure 1). Mutagenesis studies have shown that the two NH_2-terminal basic residues in this helix (R96 and K98 in yeast cofilin) are essential for both actin monomer and actin filament interactions of cofilin/ADF (*28*, *39*). Other studies also suggested that residues in the COOH-terminal half of the long α-helix would play an important role in actin interactions in cofilin/ADF proteins (*29*, *30*). We have previously introduced mutations at this particular region of the yeast cofilin gene and shown that, unlike other mutations that disrupt actin interactions of cofilin, these mutations do not result in an abnormal growth phenotype in yeast (*28*). To test the role of this region in actin binding, we produced mutant proteins Cof1−18p (K105A/D106A) and Cof1−19p (R109A/R110A) as well as charge reversal mutant Cof1−30p (R109E/R110E) in *E. coli* and examined the actin binding properties of these three yeast cofilins which carry mutations in this region.

Measurements of circular dichroism spectra show that the three doublets of point mutations do not cause a significant difference in the α-helical content of cofilin (data not shown). The differences in melting points between two mutant cofilins (T_m = 62 °C for Cof1−18p and T_m = 63 °C for Cof1−19p) and wild-type cofilin (T_m = 64 °C) are within experimental error. However, charge reversal mutations

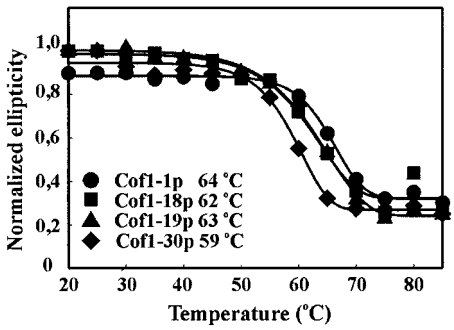

FIGURE 2: Temperature denaturation studies on wild-type and mutant cofilins. Melting points were measured by following the CD signal at 222 nm as the temperature was increased in 5 °C intervals. Wild-type and Cof1−18p and Cof1−19p mutant cofilins unfold at 62−64 °C, whereas the charge reversal mutant cofilin (Cof1−30p) unfolds at 59 °C. All plots are normalized averages of three independent measurements.

(R109E/R110E) in the long α-helix result in a detectable decrease in the stability of yeast cofilin (T_m = 59 °C for Cof1−30p) (Figure 2). This indicates that none of these mutations significantly alters the three-dimensional structure of yeast cofilin, but that the charge reversal mutations result in a small decrease in the stability of yeast cofilin.

The Highly Conserved Charged Residues in the COOH-Terminal Half of the Long α-Helix Are Not Essential for F-Actin Binding in Yeast Cofilin. We first carried out an actin filament cosedimentation assay to examine whether the charged residues in the COOH-terminal half of α-helix 3 participate in F-actin binding. In this assay as well as in all but one subsequent assay (see below), we used purified yeast actin. This way, all organism-specific inconsistencies are excluded because there is only one isoform of actin and cofilin in yeast. In cosedimentation assays, we used a constant cofilin concentration of 1 μM and varied the concentration (0, 2, 3, or 4 μM) of prepolymerized actin filaments. At pH 7.5, the wild-type yeast cofilin, as well as Cof1−18p, Cof1−19p, and Cof1−30p mutant cofilins, exhibited practically identical binding curves in the actin filament cosedimentation assay (Figure 3B). It is important to note that the cofilin mutants in our previous studies, which resulted in a temperature sensitive or lethal phenotype in yeast due to defects in actin filament interactions, exhibited binding curves dramatically altered compared to that of wild-type cofilin under similar experimental conditions (*28*). This indicates that the residues mutated in Cof1−18p (K105 and D106) as well as Cof1−19p and Cof1−30p (R109 and R110) are not important for F-actin binding in yeast cofilin.

The Long α-Helix of Yeast Cofilin Is Involved in G-Actin Binding. In our actin filament cosedimentation assays, we noticed that although Cof1−19p mutant cofilin binds to actin filaments with an affinity similar to that of wild-type cofilin, it is somewhat less efficient in shifting actin from the pellet to the supernatant fraction (Figure 3A). This indicates that Cof1−19p may have defects in actin monomer interactions. To compare the actin monomer sequestering activities of wild-type and mutant cofilins at pH 7.5, we carried out an actin filament sedimentation assay with 1 μM actin and 2 μM cofilin. This assay probably reflects the ability of cofilin to bind and/or sequester ADP-bound actin monomers under physiological ionic strength conditions. In this assay, the wild-type cofilin and Cof1−18p increased the concentration

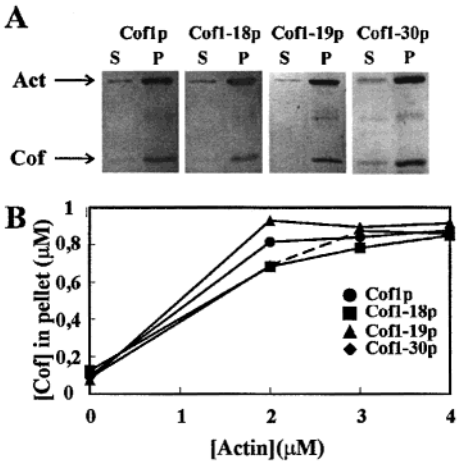

FIGURE 3: Cosedimentation assay for wild-type and mutant yeast cofilins with yeast actin at pH 7.5. Wild-type cofilin, Cof1−18p, Cof1−19p, and Cof1−30p (dashed line) interact equally well with yeast F-actin at pH 7.5. Examples of cosedimentation carried out with 4 μM actin are shown in panel A, and the mean values of three independent cosedimentation experiments are plotted in panel B. The cofilin concentration in these assays was 1 μM, and the actin concentration was varied from 0 to 4 μM.

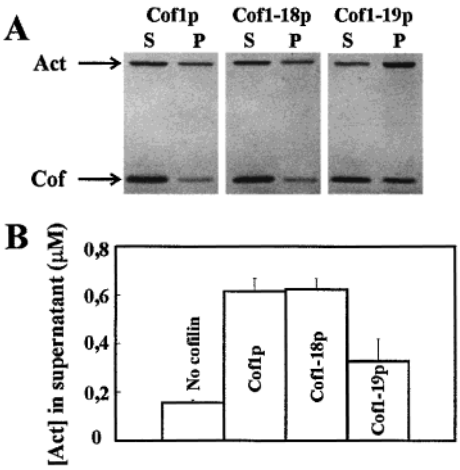

FIGURE 4: Actin monomer sequestering assay for yeast wild-type cofilin, Cof1−18p, and Cof1−19p. Wild-type cofilin and Cof1−18p increase efficiently the concentration of actin in the supernatant (from 0.15 to 0.65 μM), whereas Cof1−19p is less efficient in increasing the concentration of monomeric actin (from 0.15 to 0.35 μM). Cofilin and actin concentrations were 2 and 1 μM, respectively. Examples of representative gels are shown in panel A, and mean values from four independent measurements are plotted in panel B.

of actin in the supernatant from 0.15 to 0.6 μM, whereas Cof1−19p increased the concentration of actin in the supernatant only from 0.15 to 0.35 μM (Figure 4B).

We next compared the binding of wild-type yeast cofilin and Cof1−19p to yeast actin monomers by an assay for inhibition of nucleotide exchange on actin monomers. When bound to actin monomers, cofilin inhibits the spontaneous nucleotide exchange on actin (*14*, *15*). The inhibition of the spontaneous nucleotide exchange can therefore be applied for measuring the formation of a complex of cofilin and actin monomers. We examined the inhibition of the nucleotide exchange by fluorescence spectroscopy following the time course of ϵ-ATP incorporation into yeast actin. This assay was carried out under low-salt conditions and in the presence of $CaCl_2$, and it therefore reflects the affinity of cofilin for

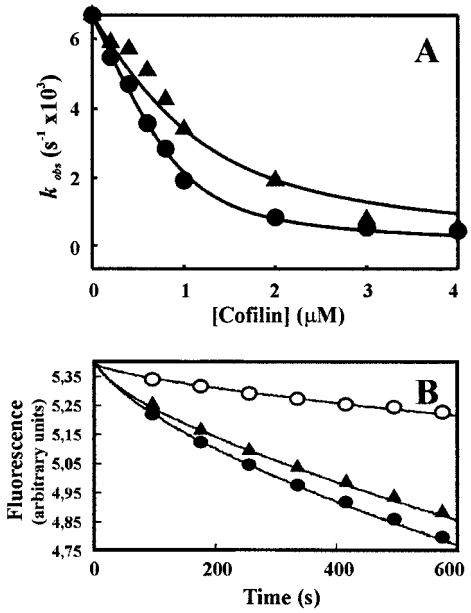

FIGURE 5: Actin monomer binding and filament depolymerization assays for wild-type (●) and Cof1−19p mutant cofilin (▲). (A) Interaction of cofilins with ATP-bound actin monomers was assessed by the inhibition of actin nucleotide exchange. The vertical axis denotes k_{obs} rates, and the horizontal axis denotes the concentration of cofilins. (B) The turnover of rabbit muscle actin filaments in the presence [wild type (●) and Cof1−19p (▲)] and absence (○) of cofilins was followed by the release of ϵ-ATP from the filaments at pH 8.0 after an ATP chase. The decrease in the fluorescence of F-actin-bound ϵ-ATP represents the turnover of actin filaments.

ATP-bound actin monomers at low ionic strengths. Wild-type cofilin promotes a strong inhibition of the nucleotide exchange, and with 2 μM cofilin, the inhibition is almost saturated (Figure 5A). In contrast, Cof1−19p is less efficient in inhibiting the spontaneous nucleotide exchange on actin monomers, and the inhibition is not saturated with 2 μM Cof1−19p. K_D values for these cofilin−G-actin complexes were calculated as described in Experimental Procedures. Wild-type cofilin binds ATP-bound actin monomers under low-salt conditions with an affinity (K_D = 0.15 μM) more than 3-fold higher than that of Cof1−19p mutant cofilin (K_D = 0.52 μM). Cof1−19p also exhibited weaker complex formation with Mg^{2+}ADP- and Mg^{2+}ATP-bound actin monomers on a native gel electrophoresis assay than wild-type cofilin (data not shown), further suggesting that this mutation indeed weakens the interaction between actin monomers and cofilin.

We also examined the effect of these mutations on the actin filament turnover by following the release of actin-bound ϵ-ATP from filaments (Figure 5B). In this assay, we used purified rabbit muscle actin instead of yeast actin. Both wild-type and Cof1−19p mutant cofilin efficiently increase the rate of actin filament turnover. Although Cof1−19p is slightly less efficient in promoting actin filament turnover in this assay, these data suggest that mutations in the COOH-terminal region of the long α-helix do not result in significant defects for the actin filament depolymerization activity of yeast cofilin.

PIP_2-Binding Interface of Yeast Cofilin. The actin filament binding and depolymerization activities of several cofilin/ADF proteins are inhibited by phosphatidylinositide phosphates (*21*, *30*). To reveal the most potent phospholipid ligand for yeast cofilin, we screened a number of different lipids with wild-type yeast cofilin. In this assay, we also included a phosphatidylinositide headgroup to clarify whether the fatty acid chains are required for the interaction. The phospholipid binding was examined by a native gel electrophoresis assay as described by Gungabissoon et al. (*22*). In this assay, cofilin was loaded on a native polyacrylamide

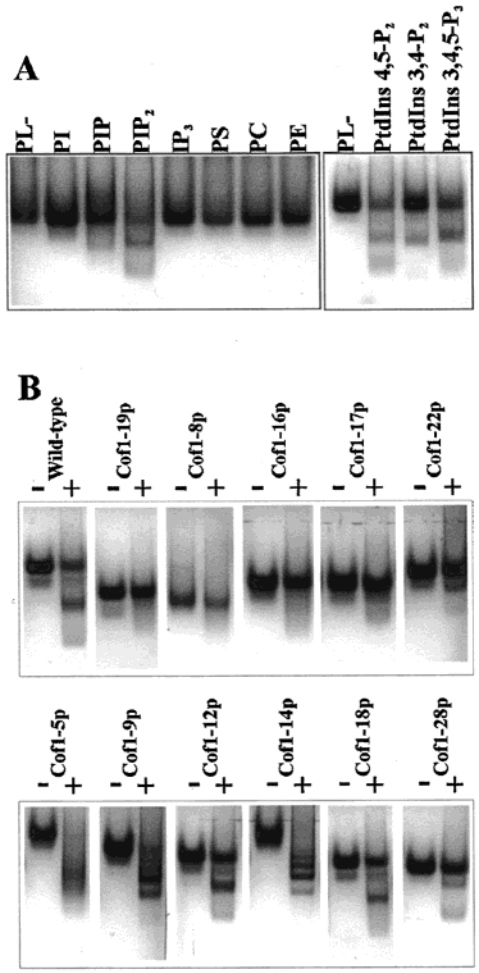

FIGURE 6: Interaction of wild-type and mutant cofilins with phospholipids. (A) Native gel electrophoresis assay for detecting the interaction of wild-type yeast cofilin with different phospholipids and a phospholipid headgroup. PI(4,5)P_2 and PI(3,4,5)P_3, and, to a lesser extent, PI(3,4)P_2 and PI(4)P, cause cofilin to move more rapidly toward the anode, indicating a net increase in the negative charge and binding interaction. PL− denotes a wild-type cofilin sample without any phospholipid, and PS, PC, and PE denote phosphatidylserine, phosphatidylcholine, and phosphatidylethanolamine, respectively. (B) A collection of yeast cofilin mutants from the systematic alanine scanning mutagenesis were tested for binding to PIP_2. The proteins were loaded on gels either alone (−) or as a 1:5 mixture with PI(4,5)P_2 (+). The following mutants were included in this assay: Cof1−18p (K105A/D106A), Cof1−19p (R109A/R110A), Cof1−28p (M1−G5 deletion), Cof1−5p (D10A/E11A), Cof1−8p (K23A/K24A/K26A), Cof1−9p (D34A/K36A/E38A), Cof1−12p (E55A/K56A), Cof1−14p (D68A/E70A/E72A), Cof1−16p (R80A/K82A), Cof1−17p (R96A/K98A), and Cof1−22p (E134A/R135A/R138A). Wild-type cofilin and six of the mutants (Cof1−5p, Cof1−9p, Cof1−12p, Cof-1−14p, Cof1−18p, and Cof1−28p) exhibited a clear shift in mobility when mixed with PIP_2. Five mutant cofilins (Cof1−19p, Cof1−8p, Cof1−16p, Cof1−17p, and Cof1−22p) did not exhibit a shift in mobility when loaded on gel toghether with PIP_2, suggesting that these mutants do not interact strongly with PIP_2.

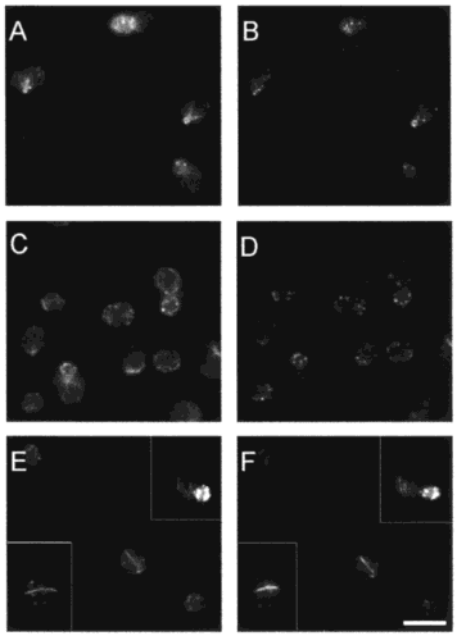

FIGURE 7: Immunofluorescence microscopy of wild-type yeast and *cof1−18* and *cof1−19* mutant strains: (A and B) wild-type yeast, (C and D) the *cof1−18* strain, and (E and F) the *cof1−19* strain. Cells were stained with an anti-actin antibody (A, C, and E) and with an anti-cofilin antibody (B, D, and F). Actin bars and/or rods are seen in approximately 3% of the *cof1−19* cells, whereas these abnormal actin structures are never found in wild-type or *cof1−18* cells. In cells displaying abnormal actin rods, cofilin staining is occasionally also seen in the cytoplasmic actin cablelike structures. The bar is 5 μm.

gel either alone or in the presence of the desired phospholipid. A shift in the electrophoretic mobility of cofilin in the presence of a phospholipid indicates a binding interaction. Although this is not a quantitative assay, we can estimate that the strength of the interaction of yeast cofilin with different lipids decreases in the following order: $PI(4,5)P_2 = PI(3,4,5)P_3 > PI(3,4)P_2 > PI(4)P$ (Figure 6A). It is important to note that IP_3, the polar headgroup of $PI(4,5)P_2$, did not alter the electrophoretic mobility of yeast cofilin in this assay. This suggests that in addition to the polar headgroup, the fatty acid part of PIP_2 also contributes to the interaction with cofilin. However, it is also possible that cofilin binds IP_3, but a shape change of the complex compensates for the alteration in the charge in the electrophoretic mobility.

To map the PIP_2-binding interface of yeast cofilin, we tested purified Cof1−18p and Cof1−19p as well as nine other charged-to-alanine yeast cofilin mutants for $PI(4,5)P_2$ binding by using the native gel electrophoresis assay. These 11 mutants are relatively evenly distributed over the surface of yeast cofilin, and therefore represent a significant coverage of the molecular surface. A list of the mutants is given in the legend of Figure 6. Six of 11 mutants tested in this study exhibited a shift in the electrophoretic mobility when loaded on gel together with $PI(4,5)P_2$, suggesting that these specific mutant cofilins can form a complex with $PI(4,5)P_2$. However, Cof1−19p (R109A/R110A) and four other charged-to-alanine cofilin mutants [Cof1−8p (K23A/K24A/K26A), Cof1−16p (R80A/K82A), Cof1−17p (R96A/K98A), and Cof1−22p (E134A/R135A/R138A)] do not form extra bands in native gel when mixed with a 5-fold molar excess of $PI(4,5)P_2$ (Figure 6B). This suggests that these five mutant cofilins no longer interact strongly with $PI(4,5)P_2$.

Phenotypes of cof1−18 and cof1−19 Yeast Cells. Although *cof1−18* and *cof1−19* mutants do not result in an altered growth phenotype in haploid yeast (*28*), we decided to test whether these mutants would cause any defects in the organization of the actin cytoskeleton in yeast cells. The haploid cells in which the wild-type copy of the cofilin gene has been replaced with either *cof1−18* or *cof1−19* mutant cofilin were grown at 30 °C to a logarithmic phase. These cells express almost identical amounts of cofilin relative to each other, as judged from a quantitative Western blot experiment (data not shown). Cells were fixed with formaldehyde after which actin and cofilin were visualized with polyclonal antibodies. Wild-type yeast cells and *cof1−18* mutant cells show normal organization of the actin cytoskeleton, and in these cells, cofilin localizes to cortical actin patches (Figure 7). In *cof1−19* cells, however, thick actin bars and/or rods are often found. These abnormal actin structures are visible in approximately 3% of the cell population in *cof1−19* mutant cells but never seen in our wild-type or *cof1−18* mutant cells. It is also interesting to note that in *cof1−19* cells cofilin localizes strongly to these actin rods and also weakly to cablelike actin structures, though the latter are only scarcely visible in the *cof1−19* mutant strain (Figure 7E,F).

DISCUSSION

The most highly conserved region in cofilin/ADF proteins is located along the long α-helix (helix 3 in yeast cofilin). The NH_2-terminal basic residues in this α-helix have been shown to be essential for actin monomer, actin filament, and PIP_2 interactions of cofilin/ADF proteins (*28*, *39*). Recent mutagenesis and peptide binding studies on *Acanthamoeba* actophorin also suggested that the charged residues in the COOH-terminal half of this α-helix would play an important role in actin filament interactions (*30*). In contrast to studies by Van Troys et al. (*30*), we show here that the corresponding charged residues in the COOH-terminal region of helix 3 in yeast cofilin are not important for actin filament binding. It is possible that the differences between these two studies can be explained by small structural differences between actophorin and yeast cofilin (*26*, *27*). However, it is also important to note that the mutagenesis strategy used in our study and that used in the study by Van Troys et al. (*30*) were different. We used charged-to-alanine mutations to neutralize the charged residues, whereas Van Troys et al. (*30*) used charge reversal mutations (e.g., lysine to glutamate). It is possible that although the charged residues in the COOH-terminal region of cofilin/ADF or actophorin do not play a central role in actin filament interactions, the replacement of these basic residues with glutamates would affect protein structure and stability. In support to this, we found that replacement of the two highly conseved arginines (R109 and R110) in yeast cofilin with glutamates results in a decrease in the melting point (from 64 to 59 °C). It is also important to note that the charge reversal mutants in the study by Van Troys et al. (*30*) unfolded at a significantly lower urea concentration than wild-type actophorin, further suggesting that charge reversal mutations in the long α-helix affect protein stability and structure.

Although the charged residues at the COOH-terminal half of the long α-helix are not important for actin filament binding in yeast cofilin, our data show that a mutation in this region (R109A/R110A) results in a small defect in actin monomer binding. This suggests that cofilin may adopt a slightly different orientation with respect to actin when bound to monomers and when bound to filaments. The role of residues R109 and R110 in actin monomer interactions is also supported by the molecular modeling studies by Wriggers et al. (*40*), in which the authors used molecular dynamics simulation to dock cofilin into actin monomers. These studies also suggested that cofilin binds to actin monomers through a similar interface with gelsolin segment 1. The similarities in cofilin−actin monomer and segment 1−actin monomer interactions are also supported by yeast two-hybrid studies, which showed that residues in actin subdomains 1 and 3 are essential for cofilin binding to actin monomers (*34*). In addition to the regions in actin subdomains 1 and 3, electron microscopy helical reconstruction studies of cofilin-decorated actin filaments (*17*) as well as studies with synthetic peptides (*41*) suggested that regions in actin subdomain 2 would be important for cofilin's interaction with actin filaments.

A number of studies have demonstrated that the actin-related activities of cofilin/ADF can be inhibited by phospholipids (*21*, *30*, *42*). PI(4,5)P_2 appears to be the most potent inhibitor of cofilin/ADF activity, but other phosphoinositides also appear to interact with cofilin/ADF (*21*, *22*). Our native gel shift assays with yeast cofilin agree with these previous studies and show that yeast cofilin binds phosphatidylinositides in a differentiating manner. Interestingly, IP_3 (Ins1,4,5-P_3) does not alter the mobility of cofilin in our assay, indicating that also the fatty acid chains are important for these interactions. Despite vigorous sonication immediately before the reaction, the lack of interaction with IP_3 could in principle be due to the inability to form vesicles or micelles, where the headgroups are aligned. The ratio of PIP_2 to other lipids and thereby the curvature of the membrane has been reported to be critical for the PIP_2 binding of some other cytoskeletal proteins (*43*).

We also used a number of yeast cofilin charged-to-alanine mutants to map the PIP_2-binding site on the cofilin molecule. On the basis of the native gel shift assay, five of the mutants did not interact strongly with PIP_2 (Figure 6B). Two of these mutants correspond to residues that in other organisms have been shown to be important for PIP_2 binding (*30*, *42*). These two mutations [Cof1−17p (R96A/K98A), and Cof1−19p (R109A/R110A)] are located at the highly conserved long α-helix of yeast cofilin. The three other mutations that disrupt the interactions with PIP_2 are located in other regions of yeast cofilin, and therefore, our results extend the previously defined PIP_2-binding interface of cofilin/ADF (Figure 8). Yeast cofilin is a polar molecule and has a positively charged surface at one face of the molecule (*26*). The five mutants defective in interactions with PIP_2 consist of clusters of residues scattered on the positively charged face of the yeast cofilin molecule (Figure 8). Because these residues are located quite far from each other on the three-dimensional structure of cofilin, it seems unlikely that yeast cofilin would have only one specific PIP_2-binding site. We therefore propose that cofilin simultaneously interacts with more than one PIP_2 molecule or, alternatively, that the interaction with PIP_2 is dynamic and would not take place in a specific site on cofilin. It is also important to note that the PIP_2-binding site(s) of yeast cofilin overlap with the areas that are important for actin binding (Figure 8). This explains why PIP_2 inhibits the actin-related activities of cofilin/ADF proteins.

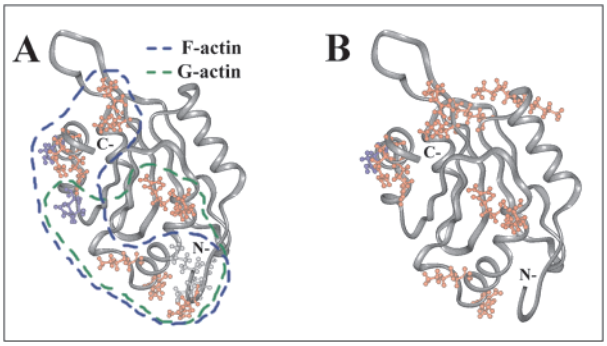

FIGURE 8: PIP_2- and actin-binding sites of yeast cofilin. (A) Molecular model for the F-actin and G-actin binding sites of yeast cofilin. The F-actin binding site and G-actin binding sites are circled by blue and green dashed lines, respectively. Lysines and arginines are colored red, aspartates and glutamates blue, and the neutral amino acids in the mutated clusters gray. N- and C-termini of the cofilin molecule are denoted with letters. (B) Molecular model indicating the positions of yeast cofilin residues that are important for PIP_2 binding. The residues involved in PIP_2 interactions are scattered on the positively charged face of the cofilin molecule. It is important to note that the binding sites for actin and PIP_2 overlap with each other on the cofilin molecule.

Yeast cells expressing *cof1−19* mutant gene have some abnormalities in their actin cytoskeleton (Figure 7). The cortical actin cytoskeleton in these cells looks rather normal, but approximately 3% of the cells have long cytoplasmic actin bars reaching from one end of the cell to the other. Such actin structures are never seen in wild-type yeast cells under similar growth conditions. Our biochemical studies showed that in addition to defects in PIP_2 interactions, Cof1−19p has a modest defect in actin monomer binding activity. It has also been reported that in *cof1−19* cells the localization of another component of the cortical actin cytoskeleton, Aip1p, is abnormal (*34*). At this point, it is difficult to judge whether the phenotype in *cof1−19* cells results from defects in actin monomer, PIP_2, or Aip1p interactions. It is important to note, however, that despite the defect of Cof1−19p in PIP_2 binding, the *cof1−19* cells are still viable. Therefore, our results suggest that strong PIP_2 binding activity of cofilin is not crucial for viability in yeast. Previous studies have demonstrated that the actin filament binding and depolymerization activities are essential functions of yeast cofilin (*3*). It is also important to note that actin rods similar to those observed in *cof1−19* cells were shown to form in neurons in which a nonphosphorylated form of cofilin/ADF is expressed (*44*). Because yeast cofilin activity appears not to be downregulated by phosphorylation, it is possible that PIP_2 binding downregulates cofilin activity in yeast.

As a conclusion, we demonstrated that the highly conserved charged residues in the COOH-terminal region of helix 3 in yeast cofilin are not critically involved in actin filament binding. Interestingly, mutations in these residues result in defects in actin monomer interactions. Furthermore, we mapped the PIP_2-binding interface of yeast cofilin and show that it overlaps with actin monomer and actin filament binding sites of cofilin.

ACKNOWLEDGMENT

We thank Dr. Chang-Jie Jiang for advice concerning the native electrophoresis lipid binding assay, Dr. Roman Tuma for his help with the fitting equation, and Dr. Helena Aitio for her help with CD experiments. Drs. Alan Weeds, Petri Auvinen, and Harri Savilahti are acknowledged for valuable comments on the manuscript.

REFERENCES

1. Bamburg, J. R., Harris, H. E., and Weeds, A. G. (1980) *FEBS Lett. 121*, 178−181.
2. Carlier, M.-F., Laurent, V., Santolini, J., Melki, R., Didry, D., Xia, G.-X., Hong, Y., Chua, N.-H., and Pantaloni, D. (1997) *J. Cell Biol. 136*, 1307−1323.
3. Lappalainen, P., and Drubin, D. G. (1997) *Nature 388*, 78−82.
4. Rosenblatt, J., Agnew, B. J., Abe, H., Bamburg, J. R., and Mitchison, T. J. (1997) *J. Cell Biol. 136*, 1323−1332.
5. Abe, H., Obinata, T., Minamide, L. S., and Bamburg, J. R. (1996) *J. Cell Biol. 132*, 871−885.
6. Gunsalus, K. C., Bonaccorsi, S., Williams, E., Verni, F., Gatti, M., and Goldberg, M. L. (1995) *J. Cell Biol. 131*, 1243−1259.
7. Chen, J., Godt, D., Gunsalus, K., Kiss, I., Goldberg, M., and Laski, F. A. (2001) *Nat. Cell Biol. 3*, 204−209.
8. Moon, A. L., Janmey, P. A., Louie, K. A., and Drubin, D. G. (1993) *J. Cell Biol. 120*, 421−435.
9. Iida, K., Moriyama, K., Matsumoto, S., Kawasaki, H., Nishida, E., and Yahara, I. (1993) *Gene 124*, 115−120.
10. Aizawa, H., Sutoh, K., Tsubuki, S., Kawashima, S., Ishii, A., and Yahara, I. (1995) *J. Biol. Chem. 270*, 10923−10932.
11. Ono, S., Baillie, D. L., and Benian, G. M. (1999) *J. Cell Biol. 145*, 491−502.
12. Maciver, S. K., and Weeds, A. G. (1994) *FEBS Lett. 347*, 251−256.
13. Ressad, F., Didry, D., Xia, G., Hong, Y., Chua, N., Pantaloni, D., and Carlier, M.-F. (1998) *J. Biol. Chem. 273*, 20894−20902.
14. Hawkins, M., Pope, B., Maciver, S. K., and Weeds, A. G. (1993) *Biochemistry 32*, 9985−9993.
15. Hayden, S. M., Miller, P. S., Brauweiler, A., and Bamburg, J. R. (1993) *Biochemistry 32*, 9994−10004.
16. Galkin, V. E., Orlova, A., Lukoyanova, N., Wriggers, W., and Egelman, E. H. (2001) *J. Cell Biol. 153*, 75−86.
17. McGough, A., Pope, B., Chiu, W., and Weeds, A. G. (1997) *J. Cell Biol. 138*, 771−781.
18. Maciver, S. K. (1998) *Curr. Opin. Cell Biol. 10*, 140−144.
19. Du, J., and Frieden, C. (1998) *Biochemistry 37*, 13276−13284.
20. Chan, A. Y., Bailly, M., Zebda, N., Segall, J. E., and Condeelis, J. S. (2000) *J. Cell Biol. 148*, 531−542.
21. Yonezawa, N., Nishida, E., Iida, K., Yahara, I., and Sakai, H. (1990) *J. Biol. Chem. 265*, 8382−8386.
22. Gungabissoon, R. A., Jiang, C.-J., Drøbak, B. K., Maciver, S. K., and Hussey, P. (1998) *Plant J. 16*, 689−696.
23. Moon, A., and Drubin, D. G. (1995) *Mol. Biol. Cell 6*, 1423−1431.
24. Agnew, B. J., Minamide, L. S., and Bamburg, J. R. (1995) *J. Biol. Chem. 270*, 17582−17587.
25. Hatanaka, H., Ogura, K., Moriyama, K., Ichikawa, S., Yahara, T., and Inagaki, F. (1996) *Cell 85*, 1047−1055.
26. Fedorov, A. A., Lappalainen, P., Fedorov, E. V., Drubin, D. G., and Almo, S. C. (1997) *Nat. Struct. Biol. 4*, 366−369.
27. Leonard, S., Gittis, A., Petrella, E., Pollard, T., and Lattman, E. (1997) *Nat. Struct. Biol. 4*, 369−373.
28. Lappalainen, P., Fedorov, E. V., Fedorov, A. A., Almo, S. C., and Drubin, D. G. (1997) *EMBO J. 16*, 5520−5530.
29. Yonezawa, N., Nishida, E., Ohba, M., Seki, M., Kumagai, H., and Sakai, H. (1989) *Eur. J. Biochem. 183*, 235−238.
30. Van Troys, M., Dewitte, D., Verschelde, J. L., Goethals, M., Vandekerckhove, J., and Ampe, C. (2000) *Biochemistry 39*, 12181−12189.
31. Higuchi, R., Krummel, B., and Saiki, R. K. (1988) *Nucleic Acids Res. 16*, 7351−7367.
32. Ausubel, F. M., Brent, R., Kingston, R. E., Moore, D. D., Seidman, J. G., Smith, J. A., and Struhl, K. (1990) *Current Protocols in Molecular Biology*, John Wiley and Sons, New York.
33. Zechel, K. (1980) *Eur. J. Biochem. 110*, 343−348.
34. Rodal, A. A., Tetreault, J. W., Lappalainen, P., Drubin, D. G., and Amberg, D. C. (1999) *J. Cell Biol. 145*, 1251−1264.
35. Spudich, J. A., and Watt, S. (1971) *J. Biol. Chem. 246*, 4866−4871.
36. Safer, D. (1989) *Anal. Biochem. 178*, 32−37.
37. Ayscough, K. R., and Drubin, D. G. (1998) in *Cell Biology, A Laboratory Handbook*, Academic Press, San Diego.
38. Laemmli, U. K. (1970) *Nature 277*, 680−685.
39. Moriyama, K., Yonezawa, N., Sakai, H., Yahara, I., and Nishida, E. (1992) *J. Biol. Chem. 267*, 7240−7244.
40. Wriggers, W., Tang, J. X., Azuma, T., Marks, P. W., and Janmey, P. A. (1998) *J. Mol. Biol. 282*, 921−932.
41. Renoult, C., Ternent, D., Maciver, S. K., Fattoum, A., Astier, C., Benyamin, Y., and Roustan, C. (1999) *J. Biol. Chem. 274*, 28893−28899.
42. Yonezawa, N., Homma, Y., Yahara, I., Sakai, H., and Nishida, E. (1991) *J. Biol. Chem. 266*, 17218−17221.
43. Tuominen, E. K., Holopainen, J. M., Chen, J., Prestwich, G. D., Bachiller, P. R., Kinnunen, P. K., and Janmey, P. A. (1999) *Eur. J. Biochem. 263*, 85−92.
44. Minamide, L. S., Striegl, A. M., Boyle, J. A., Meberg, P. J., and Bamburg, J. R. (2000) *Nat. Cell Biol. 9*, 628−636.

BI0117697